Fast ultra-deep silicon cavities : Toward Isotropically Etched Spherical Silicon molds using an ICP-DRIE

Etienne Herth[1,2], Maciej Baranski[2], Djaffar Berlharet[2], Samson Edmond[1], David Bouville[1], Laurie Calvet [1], Christophe Gorecki[2]

1. Centre de Nanosciences et de Nanotechnologies, CNRS UMR 9001, Univ. Paris-Sud, Université Paris-Saclay, C2N-Orsay, 91405 Orsay cedex, France.
2. FEMTO-ST, Université de Franche Comté, UBFC, CNRS UMR 6174–25044 Besançon cedex, France

E-mail: etienne.herth@c2n.upsaclay.fr

July 2018

Abstract. The paper investigates the parameter optimization of isotropic bulk silicon micro-scale etching using an Inductive Coupled Plasma -Deep Reactive Ion Etching (ICP-DRIE) system. The source power, the frequency and the SF_6 (sulfur hexafluoride) gas pressure are optimized. Etch profile results and how their characteristics depend on process and feature size have been studied. We report detailed observations of the resulting for various etching parameters, covering: pressure from 30 to 70 mTorr, SF6 flow rate from 400 to 500 sccm, platen power from 20 to 150 W, and ICP power from 2000 to 2500 W. This goal here is to present how anisotropic and isotropic etch processes for a wide range of applications in micro-electro-mechanical-systems (MEMS) and Micro Optoelectronic Mechanical System (MOEMS) fabrication. A deep anisotropic etch through a 1.4 mm thick silicon wafer with smoothly etched surfaces has been achieved. Isotropic plasma etching is obtained, including a relation between the etching depth, the undercut and the normalized radius of curvature (ROC) of the profile. The choice of using photoresist masks provides a better flexibility and economical processing. The presented results can be valuable for a wide range of applications, thus allowing a massive production using only a single commercial ICP DRIE tool, low cost and compatible with an industrial perspective.

Keywords : silicon, ICP-DRIE, ROC, mold, microfluidics, microlenses.

Submitted to: *J. Micromech. Microeng.*

1. Introduction

Microsystems technologies are widely used in manufacturing and laboratory research. Today, mainstream microelectronic and microtechnology predominantly use silicon as the substrate material. In that way, the Inductive Coupled Plasma (ICP) reactor has been thus widely used for anisotropic silicon etching because it is abble to obtain a high aspect ratio, while maintaining a vertical side wall [1, 2, 3, 4]. Indeed, by Deep Reactive Ion Etching (DRIE) technology, the silicon substrate can be etched fairly quickly and manufactured at low cost for mass production [5]. This plasma technology is becoming increasingly attractive in a very wider array of applications [6, 7, 8, 9, 10, 11, 12] as well as for microfluidics devices [13, 14, 15, 16], microprobes [17, 18], microlens molds [19, 20, 21], roll bearings components [22] and micro-optic structures [23, 24, 25, 26, 27].

The development of advanced MOEMS and Microfluidics devices demands different shapes with planer, spherical, aspheric and free form surfaces of high profile and excellent surface finish. The design of aspheric surfaces are extremely important in optical systems (eg microlenses) and have been applied in various applications. Indeed in miniaturized system, the aspheric surfaces can correct aberrations, improve the image quality, and reduce the size and weight of optical systems. Further investigation has been done in our laboratory to manufacture microlenses mold by wet etching [19]. Isotropic etching of silicon can be done by wet chemistry or by plasma etching, however the latter has not much gained much attention compared with wet etching the isotropic in both glass [28, 29] and silicon materials. Likewise, the silicon wet etching is always used in MEMS during the final stage of the micromachining process, such as, for the release of the cantilever beam from the substrate [30, 31, 32, 33]. The elimination of optical aberration in micro-optical systems can be achieved by use of aspherical silicon molds characterized by negative conic constant, however not many micro-fabrication technologies allow arbitrary control of generated geometries of microlenses. In this respect our motivation is to combine anisotropic etching and isotropic etch in one DRIE tool. In this article we will present results on ICP-DRIE for various silicon size features as a function of ICP etch processes. This paper is organised as follows: the second section describes the process used to fabricate, characterize and compare various sizes apertures. The third section describes the ICP process for silicon cavities of millimeter range depths. In the fourth section, we investigate the isotropic effect by exploring how the shape of the silicon aperture evolves during the ICP processes. We conclude with a discussion of these investigations and its application to microfluidic, microlenses molds, and microsystem through MOEMS and BIOMEMS applications.

2. Fabrications and characterizations method

The experiments were performed in a Surface Process Technology Systems (SPTS) Rapier tool. It was used with up to 3 kW of 13.56 MHz power. The wafer chuck is cooled with water. Gases employed in this study were perfluorocyclobutane (C_4 F_8), sulfur

hexafluoride (SF_6), Argon (Ar) and oxygen (O_2) (in sccm denotes cubic centimeters per minute). An oxygen clean was performed between each experiment to remove polymer off the sidewalls of the reactor, minimize contamination, and preserve repeatability. There are numerous important etchant properties, such as the etch rate, masking materials, selectivity, surface roughness. Kovacs and al. [34] have provided a generalized comparison of the various etchants in terms of many of these important properties and the availability of suitable masking films [34]. In this work, different etch processes were studied and their general characteristics were compared. Typical parameters for these processes are tabulated in Table I. Samples were processed on standard 4 inch, 1–20 ohm.cm, silicon wafers of ⟨100⟩ orientation. Photoresist (AZ9260, 6 μm-thick), was used to pattern the test geometries and as mask material, shown in Figure 1. The cavities were etched and studied using an optical microscope and a Scanning Electron Microscope (SEM). The resulting SEM of cross sections were subsequently digitized in a manual drawing program and numerically processed in python software.

3. Anisotropic etch

In deep silicon etching for microelectromechanical system(MEMS) typical etch depths are generally 10–500 μm [35]. Using the Bosch process, very high aspect ratio trenches of up to 107:1 were reported for 374 nm widths by Marty et al. [36]. More recently, aspect ratios of 160:1 were reported by Parasuraman et al. for trenches of 250 nm widths [37]. However, for differents MEMS and MOEMS applications, we needs etch depth greater than 500 μm. There, we have target 1.4 mm depths using a mask photoresist (AZ9260) which is suitable and can be deposited with thickness more than 20 μm. The DRIE conditions are summarized in Table 1. In these experiments, the duty cycle was fixed at 10 %, its effect is important on the etching process and profile (see Figure 2), while varying the other parameters . This pre-test shown in Table 1, is focused on the coupling effect of the gas mixture, the source power and the pressure on the etching rate and profile.

As expected, it becomes evident that the etch rates are monotonically decreased with decreasing aperture size as seen in Figure 2a. This is the so-called Aspect Ratio Dependent Etching (ARDE) effect. The results of the etch profiles are carefully analyzed by the isotropic ratio [38], A_F defined as:

$$A_F = 1 - \frac{r_{lat}}{r_{vert}} \qquad (1)$$

where r_{lat} is either the horizontal dimension of the foot edge from the mask edge or the undercut rate and r_{vert} is either the vertical etched depth or the etch rate as illustrated in Figure 3.

Figure 4 shows a selection of the sidewall profiles that have been obtained in our experiments. These SEMs clearly demonstrate that it is difficult to obtain a straightforward definition of the anisotropy. Indeed, depending on the process parameters, the profiles may vary from ideal isotropy. No significant amount of undercut

was observed using the recipe 1a, which results in an anisotropy value of 1 indicating a perfect vertical sidewall with no mask undercut. Recipe 2 resulted in an anistropy close to 0.7.

In fact, at high pressures of O_2, the value of the anisotropy, as defined before, may be lower because of outward by sloping etch profiles. Previously, good results on of ultra-deep silicon cavities with smooth sidewalls, using an Alcatel DRIE reactor tool, have been reported [39] with etch rate around to 5 μm/min. However, based on the recipe 1 results, the relative etch rate with the same design rule, the rate process is higher and close to 11 μm/min with a scalloping around 250 nm. A consequence of the pulsed DRIE process with this high etch rate is improved cost, efficiency and yield of the microfabrication devices. Mastering deep etching technologies has enabled manufacturing and to miniaturization of the atomic-clock and magnetometer as highlighted in Figure 4.

Nevertheless, to completely etch through a 1.4 mm thick silicon wafer suffers the intrinsic disadvantage of scalloped sidewalls and high sidewall surface roughness. For instance,the process needs to be

one tuned for every aperture size during the same step. Recipe 1a consists of alternating isotropic etching under SF_6 plasma and passivation using the C_4F_8 plasma. When silicon is being etched using this Bosch process, silicon grass, due to the residual passivation layer, is formed at the bottom of the holes as etching by products. If, the passivation layer, after C_4F_8 deposition, is not completely removed, it makes a micromask. Silicon grasses are thus undesirable by product in micro-devices. To overcome these drawbacks, optimized recipes processes are presented in more detail in Table 2. Besides three recipes presented in table 1, gradual increase of process ecthing time on several step etch at room using presented SF_6/C_4F_8 as well as other parameter (pressures, power) presented in Table 2, proves that this approach has many special advantages e.g., smooth trench sidewall, high etch rate and selectivity.Table 2 and Figure 5 present the results for these trenches. No mask undercut was observed using recipe 1a and 1b, the surface scalloping inherent to the bosch process were around to 200 nm. The etch profile appear straight and with smooth sidewall. With revised recipe 1b, we have successfully etched trenches as narrow as 10 μm for 55 μm depth and as wide as 1100 μm for 117 μm depth.

The performance makes this method have good application potentials for the production of microelectronic and MOEMS, and MEMS in particular to completely etch through a thicker silicon wafer (more than 500 μm). The reported process was employed to fabricate cells for miniature atomic clocks [40]. The study of the undercut and the curvature profile, in the case of an anisotropy factor close to 0 (recipe 3) is considered in more depth in the next section.

4. Isotropic etch

Even though wet silicon etch can have an aspect ratio as high as 600, this deep anistropic etch technique by aqueous solutions is inherently limited to the fabrication of structures such as microlenses mold (see figure 6) where the isotropic effect is desired. In recent years, much effort has been placed on the development of advanced in isotropic wet etching [41, 42, 34, 19, 43] and in istropic dry etching [20, 21, 22]. Consequently, the spherical cavity size was found to depend mostly on the size of the etch-mask opening, and be independent of the etching time. A variety of mask materials and etching conditions were investigated to obtain a large spherical cavity (2.5 mm in radius) with good circularity and smoothness. Early works by our team focused on microlenses, which were specifically developed for the different microfabrication [19, 44] approaches in MOEMS applications [26]. Previous reports on isotropic dry etching technology have documented [20, 22] and presented that the anisotropic plasma can be optimized when the mask opening and the process parameter are matched to produce a sphere shape. Here, we considered different size of circular mask openings (ranging from 20 μm - 600 μm).

Figure 7 shows the mask undercut and the etch depth as a function of mask opening diameter. The results show that for all the test structures analyzed, the etch rate increased quite significantly with increasing pressure. The undercut and the etch depth are found to increase with mask opening, but tends to saturate between 350 μm to 600 μm diameters, which indicates that the silicon etch rate is principally limited by the availability of fluorine radicals at the silicon substrate. At high pressure, the non-uniformity of etch depth was observed. This could be attributed in large part to the limitations of the pumping system of the ICP reactor, which plays an increasingly important role in the uniformity of species diffusion inside the reactor.

While Figure 8 shows that for the different mask openings, the degree of anisotropic etching given in equation 1 is range from 0.2 to 0.4 whatever the pressure. Increasing the pressure should increase the atomic fluorine concentration and decrease the ion bombardment. Both effects lead to a reduction of the anisotropy, in agreement with our results at high pressures (100 mTorr and 150 mTorr). However, at 500 sccm SF_6 flow rate, the etch rate and undercut rate were saturated because of (a)the recombination of radicals before reaching the sample surface and /or (b) insufficient source power (2500 W) to promote the dissociation of SF_6 and produce fluorine radicals. These results show that the physical etching rate in the vertical direction increased faster than in horizontal direction when the pressure was higher than 40 mTorr. SEM of cleaved samples was utilized to confirm thes degree and the profile of this anisotropic measurements.

The Figure 9 shows SEM micrograph of the etched surface taken with a 45 °tilt for wafers etched at 40 mTorr, 100 mTorr and 150 mTorr pressure. These results show that surface roughness decreases significantly at lower pressure. Clearly, as presented in Figure 10, the curvature of the cavity is variable and depends on the mask opening and the fabrication process. For larger openings masks, the profiles show a very flat

center region. As a consequence, the degree of anisotropic etching is a good indicator and must be completed by SEM view or by interferometry measurement.

Nevertheless, a spherical profile measurements are more difficult than flat surfaces. The more complex geometries are often described as conic sections that can be expressed as following equation :

$$Z\left(r\right)=\frac{cr^2}{1+\sqrt{1-\left(k+1\right)c^2r^2}}+\sum_{i=n_0}^{N}\alpha_i r^i \tag{2}$$

where r is the radial coordinate, c is vertex curvature, α_i are the polynomials coefficients. This formulation is used in geometric optics to specify oblate elliptical k $>$ 0, spherical k = 0, prolate elliptical 0 $<$ k $<$ -1, parabolic k = -1, and hyperbolic k $<$ -1. When the paraxial approximation is valid, the optical surface can be treated as a spherical surface with the same radius.

The normalized conic constant k and the radius of curvature (ROC) of the profiles [45] were analyzed by fitting a sphere to the bottom part of the silicon cavities.

As expected, the mask opening data (see Figure 11 and Figure 12) and the conic constant k suggest that an mask opening of 10 μm to 210 μm allows a semi-circular cross-section and was therefore selected as the opening for future isotropic etching experiments for microlense molds. For larger openings masks, the ROC is higher due to the flat profile. The surface roughness increased with change in chamber pressure and was affected significantly for the largest opening masks. Furthermore, in the literature, the roughness, the size aperture and the cavity depth are spread over a wide range according to the mask opening, the process parameters and the etching time. One example of these results is summarized in Table 2. Compared with the microlenses molds [20] and microball-bearing mold [22] as is shown in Table 2, the smallest opening masks showed much low roughness. Compared with other common isotropic etching using ICP, our data suggests that an opening up to 200 μm would be able to give a semi-circular mold. The profile obtained by SEM imaging (Fig. 9b), with a diameter of 100 μm reveals that the structure can be described by conic section k = – 0.18, and ROC = 55.5 μm at 100 mTorr. With such negative conic constant are highly desirable for the construction of micro-optical scanner [26].

5. Discussion

During this DRIE study , we have investigated both anisotropic and isotropic etching processes: anisotropic etching to achieve the depth, and the isotropic etching in order to obtain the desired spherical shape. There are many parameters in the processing: pressure, coil power/ platen power, etch/passivation time ratio, flow rate of etch/passivation gas, temperature. Low process pressure (Recipe 1a) is beneficial for high-aspect ratio etching, as exchange of species in narrow deep trenches is accelerated by the higher mean-free path of the gas molecules and radicals. Recipe 1b is a trade-off with higher etch rate requirements, where the etch rate increases with higher pressure

levels. We conclude that the proposed process is suitable in order to prevent undesirable etching side effects, such as undercut or bowing and Si grasses as seen in Figure 13. However, Equation 1 does not give information whether the anisotropy is due to mask undercut, to the parameter process or the sloped profiles. It is shown that the proposed investigation in conjunction with other tools characterizations it is therefore able to predict the curvature according to the mask aperture designed and paramater process. This in turn allows using the semi-analytical solution as a very fast solver in analyzes of results. Thus, this approach plays an essential role for the particular design for replication of the microfluidic system. Further research will be forthcoming for the manufacture of microlenses where the lower roughness and a spherical curvature are essential for optimal functioning.

For the past few years, many efforts have been made to study the structures in the Bosch. We demonstrate here :

• Various demands on mask selectivity, etch rate and profile can be met in the fabrication of the silicon based on this starting point recipes.

• Fast and utlra deep etching realised at reasonably high etch rates.

• A baseline for controlling the profile of anisotropic silicon manufacturing and / or isotropic processes open a wide area of applications with one tool.

Silicon dioxide, metal masks, or even photoresist (eg AZnLOF 2020, SPR220, AZ9260) are commonly used. We propose to use a photoresist mask that is low cost approach and uses equipment, widespread in the microelectronics laboratories and industry and compatible with Roll to roll perspective.

In this work, the performed experiments were based on the anisotropic plasma toward isotropic plasma etching in order to investigate the fast ultra-deep silicon cavities of the plasma process using an ICP-DRIE but also to determine the range of structures that could be also fabricated toward isotropical plasma. Through the isotropic plasma, we demonstrated a clear potential of this technique for the generation of more complex shapes than the one that can be produced by wet-etching based techniques. In particular, we presented the possibility of creating aspherical shapes with desirable negative conic constant and high aspect ratio (and consequently high Numerical aperture NA of corresponding optical elements).

6. Conclusion

A commercially available modern plasma etch system in high frequency 13.5 MHz has been insvestigated for best performance with respect to the design goal was uses to demonstrated stable and good reliability of isotropic etching by ICP-DRIE for MEMS and MOEMS applications. A trade-off between profile and feature size can usually be found quite easily. The anisotropic silicon etch rates in ICP-DRIE reactor can reach 15 μm/min. The ICP isotropic etching technology provides an excellent alternative to release microcantilever beams and other suspended design from silicon substrate with low cost and one tool. Empirical models, which fits very well with the experimental

data, was proposed. These analyticals can serve as a basis for the design rules for the microfabrications widespread in the microelectronics, optoelectronics laboratories and industry. This study open a large scale applications which require high etch rate and stable process, controllable profile and surface properties and low costs. We are investigate the possibility to generate larger spherical shapes or structures characterized by negative conic constants that are difficult to make by use of wet etching techniques. A combination of different plasma parameters have been studied and the related ICP recipes can prove useful for optoelectronic, microelectronic and microsystem applications.

Acknowledgments

This work was partly supported by the French RENATECH network with FEMTO-ST and C2N technological facilities.

References

[1] Mita M, Mita Y, Toshiyoshi H and Fujita H 2000 *IEEJ Transactions on Sensors and Micromachines* **120** 493–497

[2] Chen S C, Lin Y C, Wu J C, Horng L and Cheng C H 2006 *Microsystem Technologies* **13** 465–474 ISSN 0946-7076, 1432-1858 URL `http://link.springer.com/article/10.1007/s00542-006-0211-2`

[3] Mita Y, Kubota M, Harada T, Marty F, Saadany B, Bourouina T and Tadashi Shibata 2006 *Journal of Micromechanics and Microengineering* **16** S135 ISSN 0960-1317 URL `http://stacks.iop.org/0960-1317/16/i=6/a=S20`

[4] Ohara J, Takeuchi Y and Sato K 2009 *Journal of Micromechanics and Microengineering* **19** 095022 ISSN 0960-1317 URL `http://stacks.iop.org/0960-1317/19/i=9/a=095022`

[5] Jansen H V, Boer M J d, Unnikrishnan S, Louwerse M C and Elwenspoek M C 2009 *Journal of Micromechanics and Microengineering* **19** ISSN 0960-1317 URL `http://dx.doi.org/10.1088/0960-1317/19/3/033001`

[6] Lavasani H, Abdolvand R and Ayazi F 2015 *IEEE Transactions on Ultrasonics, Ferroelectrics, and Frequency Control* **62** 802–813 ISSN 0885-3010

[7] Belkadi N, Baron T, Dulmet B, Robert L, Herth E and Bernard F 2015 New capacitive micro-acoustic resonators machined in single-crystal silicon stacked structures *Frequency Control Symposium the European Frequency and Time Forum (FCS), 2015 Joint Conference of the IEEE International* pp 787–792

[8] Herth E, Valbin L, Lardet-Vieudrin F and Algré E 2015 *Microsystem Technologies* 1–8 ISSN 0946-7076, 1432-1858 URL `http://link.springer.com/article/10.1007/s00542-015-2727-9`

[9] Mirjalili R, Wen H, Serrano D and Ayazi F 2015 Substrate-decoupled silicon disk resonators having degenerate gyroscopic modes with Q in excess of 1-million *2015 Transducers - 2015 18th International Conference on Solid-State Sensors, Actuators and Microsystems (TRANSDUCERS)* pp 15–18

[10] Xiong Z, Mairiaux E, Walter B, Faucher M, Buchaillot L and Legrand B 2014 *Sensors* **14** 20667–20686 URL `http://www.mdpi.com/1424-8220/14/11/20667`

[11] Song C, Wang Z, Chen Q, Cai J and Liu L 2008 *Microelectronic Engineering* **85** 1952–1956 ISSN 0167-9317 URL `http://www.sciencedirect.com/science/article/pii/S0167931708002712`

[12] Hu H C, Cheng H C, Huang T C, Chen W H, Wu S T and Lo W C 2015 On the thermal performance analysis of three-dimensional chip stacking electronic packaging with through silicon vias *2015*

International Conference on Electronics Packaging and iMAPS All Asia Conference (ICEP-IACC) pp 532–537

[13] Berthet H, Jundt J, Durivault J, Mercier B and Angelescu D 2011 *Lab on a Chip* **11** 215–223 ISSN 1473-0189 URL http://pubs.rsc.org/en/content/articlelanding/2011/lc/c0lc00229a

[14] Petralia S, Panvini G and Ventimiglia G 2015 *BioNanoScience* **5** 150–155 ISSN 2191-1630, 2191-1649 URL http://link.springer.com/article/10.1007/s12668-015-0173-x

[15] de Boer M, Tjerkstra R, Berenschot J, Jansen H, Burger G, Gardeniers J, Elwenspoek M and van den Berg A 2000 *Journal of Microelectromechanical Systems* **9** 94–103 ISSN 1057-7157

[16] Boer M J d, Tjerkstra R W, Berenschot J W, Jansen H V, Burger G J, Gardeniers J G E, Elwenspoek M and Berg A v d 2000 *Journal of Microelectromechanical Systems* **9** 94–103 ISSN 1057-7157

[17] Herwik S, Kisban S, Aarts A A A, Seidl K, Girardeau G, Benchenane K, Zugaro M B, Wiener S I, Paul O, Neves H P and Ruther P 2009 *Journal of Micromechanics and Microengineering* **19** 074008 ISSN 0960-1317 URL http://stacks.iop.org/0960-1317/19/i=7/a=074008

[18] Marzouk J, Arscott S, El Fellahi A, Haddadi K, Boyaval C, Lepilliet S, Lasri T and Dambrine G 2016 *Sensors and Actuators A: Physical* **238** 51–59 ISSN 0924-4247 URL http://www.sciencedirect.com/science/article/pii/S0924424715302041

[19] Albero J, Nieradko L, Gorecki C, Ottevaere H, Gomez V, Thienpont H, Pietarinen J, Päivänranta B and Passilly N 2009 *Optics Express* **17** 6283–6292 ISSN 1094-4087 URL http://www.osapublishing.org/abstract.cfm?uri=oe-17-8-6283

[20] Larsen K P, Ravnkilde J T and Hansen O 2005 *Journal of Micromechanics and Microengineering* **15** 873 ISSN 0960-1317 URL http://stacks.iop.org/0960-1317/15/i=4/a=028

[21] Larsen K P, Petersen D H and Hansen O 2006 *Journal of The Electrochemical Society* **153** G1051–G1058 ISSN 0013-4651, 1945-7111 URL http://jes.ecsdl.org/content/153/12/G1051

[22] Hanrahan B, Waits C M and Ghodssi R 2014 *Journal of Micromechanics and Microengineering* **24** 015021 ISSN 0960-1317 URL http://stacks.iop.org/0960-1317/24/i=1/a=015021

[23] Trupke M, Hinds E A, Eriksson S, Curtis E A, Moktadir Z, Kukharenka E and Kraft M 2005 *Applied Physics Letters* **87** 211106 ISSN 0003-6951, 1077-3118 URL http://scitation.aip.org/content/aip/journal/apl/87/21/10.1063/1.2132066

[24] Laliotis A, Trupke M, Cotter J P, Lewis G, Kraft M and Hinds E A 2012 *Journal of Micromechanics and Microengineering* **22** 125011 ISSN 0960-1317 URL http://stacks.iop.org/0960-1317/22/i=12/a=125011

[25] Xu W, Bosseboeuf A, Parrain F and Martincic E 2014 Design of a long range bidirectional MEMS scanner for a tunable 3d integrated Mirau interferometer *2014 Symposium on Design, Test, Integration and Packaging of MEMS/MOEMS (DTIP)* pp 1–6

[26] Lullin J, Bargiel S, Lemoal P, Perrin S, Albero J, Passilly N, Luc Froehly, Lardet-Vieudrin F and Gorecki C 2015 *Journal of Micromechanics and Microengineering* **25** 115013 ISSN 0960-1317 URL http://stacks.iop.org/0960-1317/25/i=11/a=115013

[27] Falgayrettes P, Gall-Borrut P, Tsigara A, Belier B and Maillard F 2015 MOEMS for near field optical microscopy: from conception to fabrication process challenges *2015 Symposium on Design, Test, Integration and Packaging of MEMS/MOEMS (DTIP)* pp 1–3

[28] Iliescu C, Jing J, Tay F E H, Miao J and Sun T 2005 *Surface and Coatings Technology* **198** 314–318 ISSN 0257-8972 URL http://www.sciencedirect.com/science/article/pii/S0257897204010990

[29] Herth E, Rolland N and Lasri T 2010 *IEEE Antennas and Wireless Propagation Letters* **9** 934–937 ISSN 1536-1225

[30] Agache V, Quévy E, Collard D and Buchaillot L 2001 *Applied Physics Letters* **79** 3869–3871 ISSN 0003-6951, 1077-3118 URL http://scitation.aip.org/content/aip/journal/apl/79/23/10.1063/1.1418031

[31] Herth E, Lardet-Vieudrin F, Valbin L and Lissorgues G 2016 Mechanical behavior of T-shaped A1n membrane based on thin film elongation acoustic resonator (IEEE) pp 1–4 ISBN 978-1-

5090-1457-6 URL http://ieeexplore.ieee.org/document/7514867/

[32] Herth E, Lardet-Vieudrin F, Deux F, Valbin L, Algré E, Schell J and Steger H 2016 Detection of out-of-plane and in-plane (XYZ) motions of piezoelectric microcantilever by 3d-Laser Doppler Vibrometry *2016 Symposium on Design, Test, Integration and Packaging of MEMS/MOEMS (DTIP)* pp 1–4

[33] Kim J S, Lee M J, Kang M S, Yoo K P, Kwon K H, Singh V R and Min N K 2009 *Thin Solid Films* **517** 3879–3882 ISSN 0040-6090 URL http://www.sciencedirect.com/science/article/pii/S004060900900162X

[34] Kovacs G T A, Maluf N I and Petersen K E 1998 *Proceedings of the IEEE* **86** 1536–1551 ISSN 0018-9219

[35] Galayko D, Kaiser A, Buchaillot L, Legrand B, Collard D and Combi C 2003 *Journal of Micromechanics and Microengineering* **13** 134 ISSN 0960-1317 URL http://stacks.iop.org/0960-1317/13/i=1/a=319

[36] Marty F, Rousseau L, Saadany B, Mercier B, Français O, Mita Y and Bourouina T 2005 *Microelectronics Journal* **36** 673–677 ISSN 0026-2692 URL http://www.sciencedirect.com/science/article/pii/S0026269205001850

[37] Parasuraman J, Summanwar A, Marty F, Basset P, Angelescu D E and Bourouina T 2014 *Microelectronic Engineering* **113** 35–39 ISSN 0167-9317 URL http://www.sciencedirect.com/science/article/pii/S0167931713005431

[38] Legtenberg R, Jansen H, Boer M d and Elwenspoek M 1995 *Journal of The Electrochemical Society* **142** 2020–2028 ISSN 0013-4651, 1945-7111 URL http://jes.ecsdl.org/content/142/6/2020

[39] Chutani R K, Hasegawa M, Maurice V, Passilly N and Gorecki C 2014 *Sensors and Actuators A: Physical* **208** 66–72 ISSN 0924-4247 URL http://www.sciencedirect.com/science/article/pii/S0924424713006298

[40] Maurice V, Rutkowski J, Kroemer E, Bargiel S, Passilly N, Boudot R, Chutani R, Galliou S, Gorecki C, Mauri L and Moraja M 2017 Microfabricated vapor cells for miniature atomic clocks based on post-sealing activated cesium dispensers *2017 Joint Conference of the European Frequency and Time Forum and IEEE International Frequency Control Symposium (EFTF/IFCS)* pp 636–637

[41] Hashimoto H, Tanaka S, Sato K, Ishikawa I, Kato S and Chubachi N 1993 *Japanese Journal of Applied Physics* **32** 2543 ISSN 1347-4065 URL http://iopscience.iop.org/article/10.1143/JJAP.32.2543/meta

[42] Han C H and Kim E S 1998 *Japanese Journal of Applied Physics* **37** 6939 ISSN 1347-4065 URL http://iopscience.iop.org/article/10.1143/JJAP.37.6939/meta

[43] Yifan Z, Sihai C, Edmond S and Bosseboeuf A 2013 *Japanese Journal of Applied Physics* **52** 076503 ISSN 1347-4065 URL http://iopscience.iop.org/article/10.7567/JJAP.52.076503/meta

[44] Albero J, Perrin S, Bargiel S, Passilly N, Baranski M, Gauthier-Manuel L, Bernard F, Lullin J, Froehly L, Krauter J, Osten W and Gorecki C 2015 *Optics Express* **23** 11702–11712 ISSN 1094-4087 URL http://www.osapublishing.org/abstract.cfm?uri=oe-23-9-11702

[45] Abdelsalam D G, Shaalan M S, Eloker M M and Kim D 2010 *Optics and Lasers in Engineering* **48** 643–649 ISSN 0143-8166 URL http://www.sciencedirect.com/science/article/pii/S0143816610000400

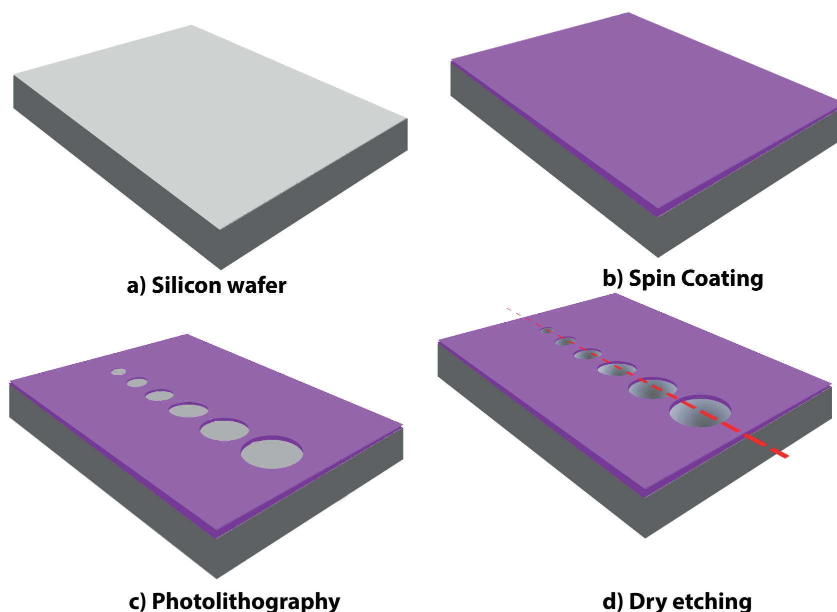

Figure 1. Flow chart of the fabrication process for the silicon microlens mold : silicon wafer, b) spin coating photoresist, c) photolithography and d) dry ecthing.

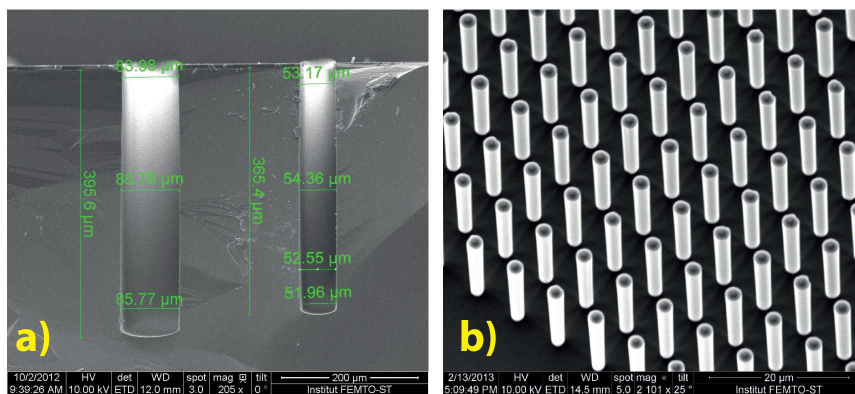

Figure 2. SEM views of typical results of a) trenches and b) pillars etched in pulsed-mode DRIE.

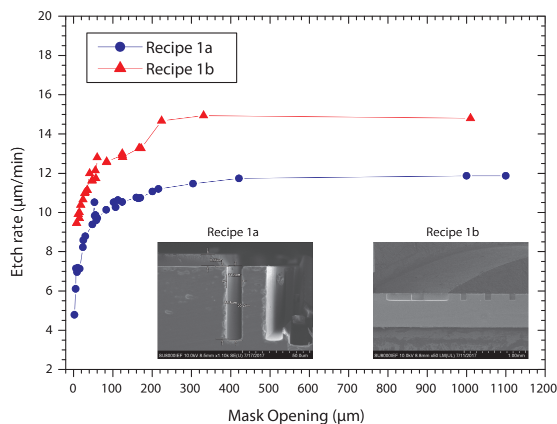

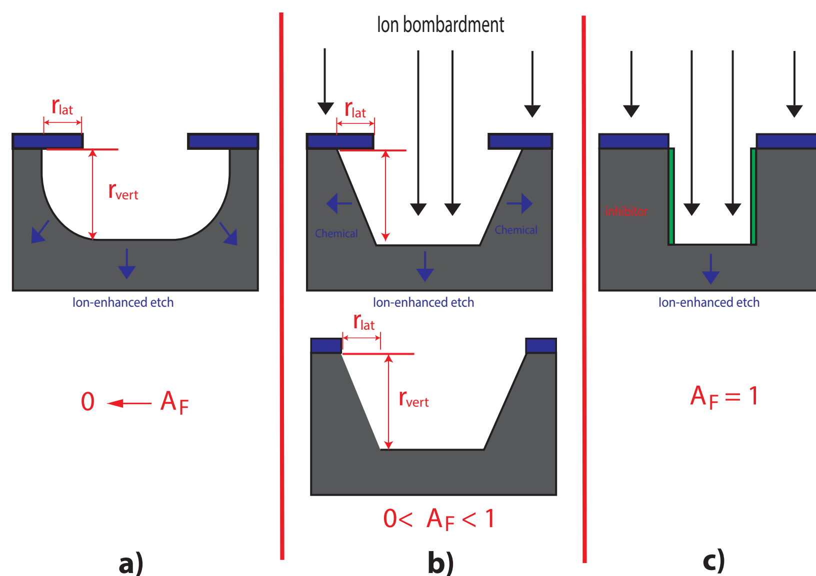

Figure 3. Profile changes as function of the silicon etching process condition: a) isotropic etch, b)directional etch and c) vertical etch .

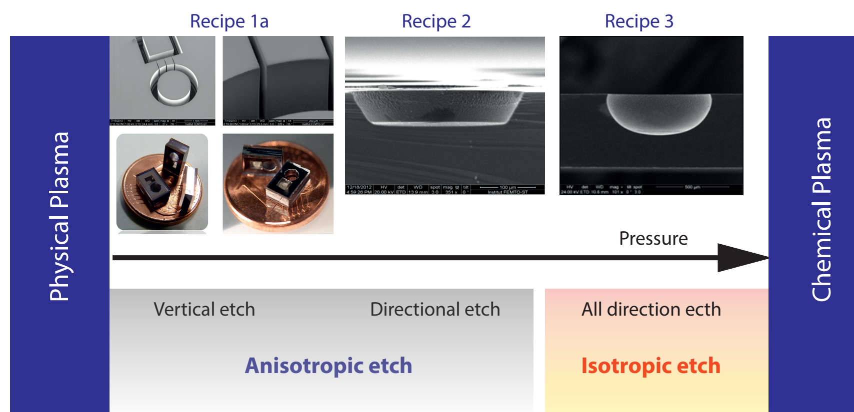

Figure 4. Illustration of typical result for pulsed-mode DRIE: physical plasma toward chemical plasma.

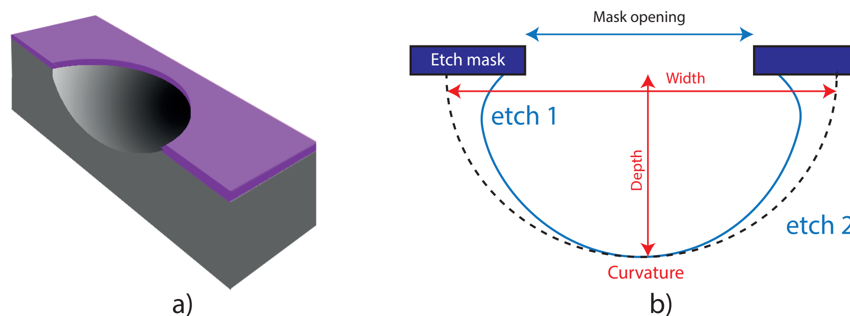

Figure 6. The etching geometry representation of the raceway profile during an ideal isotropic etch process: a) 3D design and b) geometric parameters of interest are highlighted in 2D view.

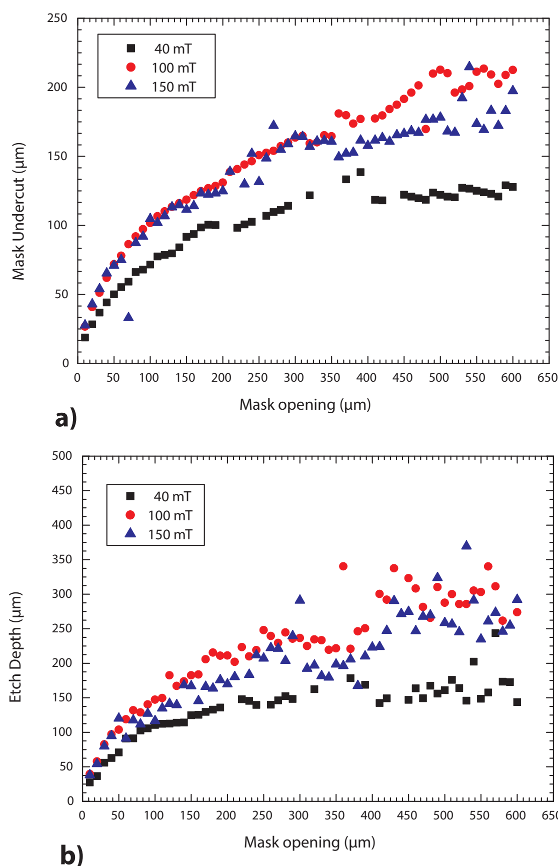

Figure 7. Silicon isotropic etching profiles as a function of plasma pressure: (a) Mask undercut, (b) Etch depth. The temperature substrate, SF_6 flow rate and time were 0C, 500 sccm, and 900 s respectively.

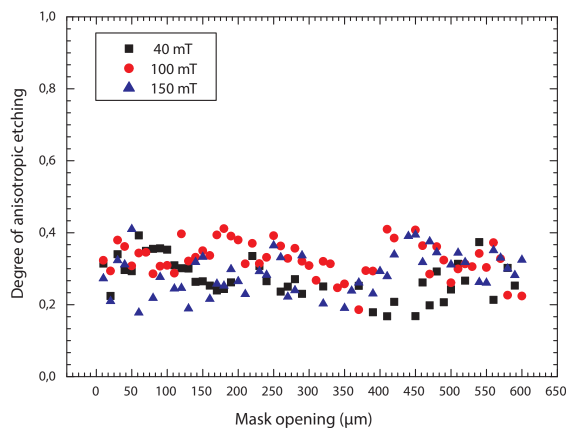

Figure 8. Degree of anisotropic etching as a function of pattern size with different plasma pressures.

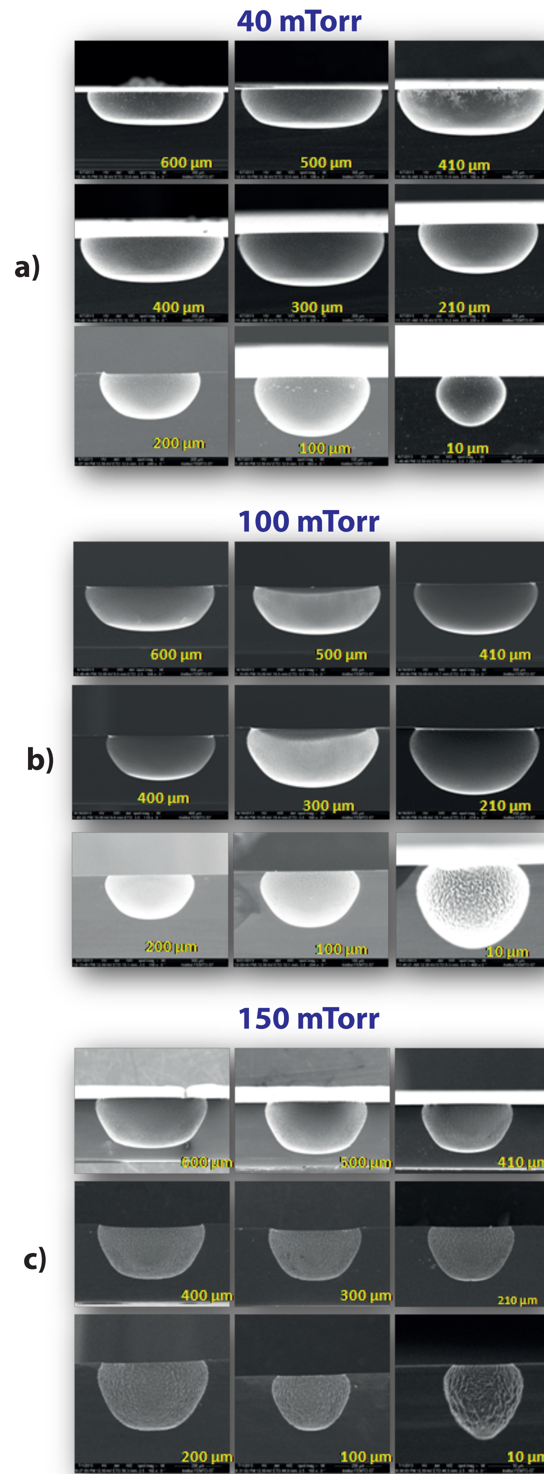

Figure 9. Cross sectional SEM micrograph of bulk-etched cavities in a ⟨100⟩ Si substrate. The parameters of the etching process were : Temperature = 0 °C, coil power = 2000 W, platen power = 20 W, SF_6 = 500 sccm standard cubic centimeters per minute (sccm) at pressure : a) 40 mtorr, b) 100 mtorr and c) 150 mtorr as indicated.

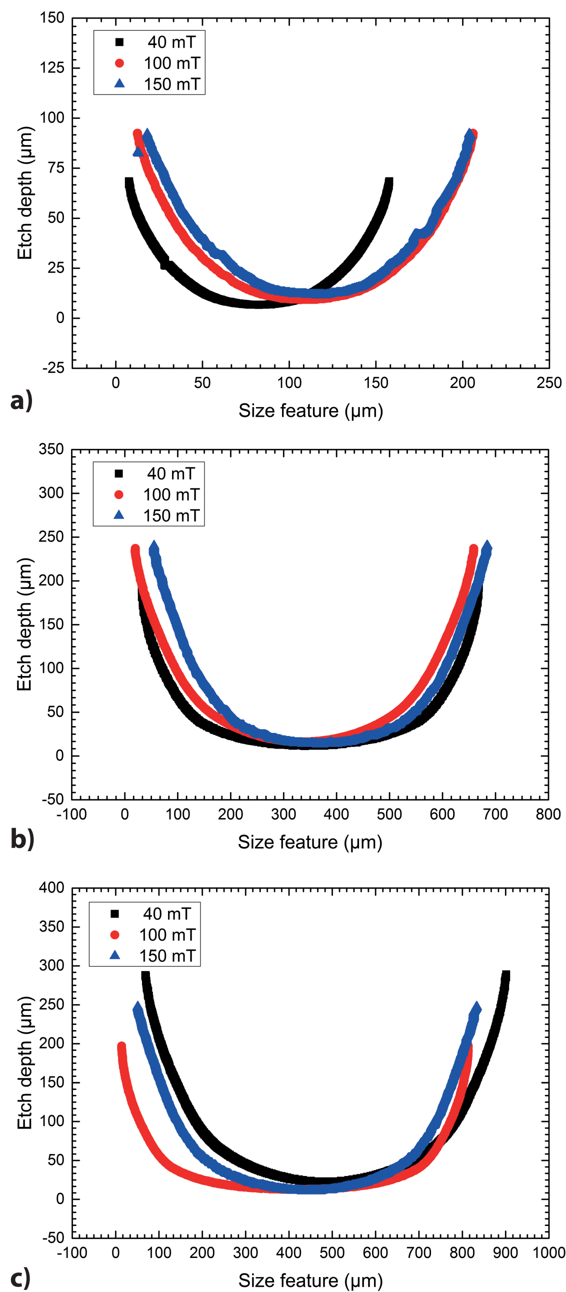

Figure 10. Comparison of the cross-sectional geometries obtained by isotropic etching for 900 s.

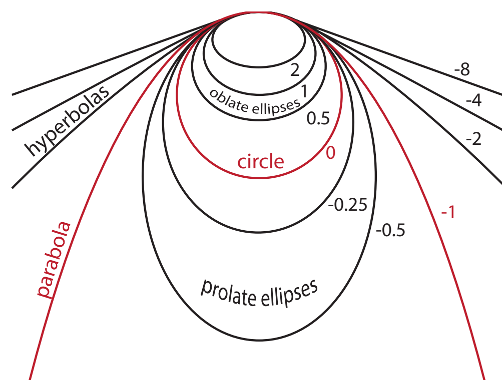

Figure 11. Profiles of conic sections with k parameter indicated.

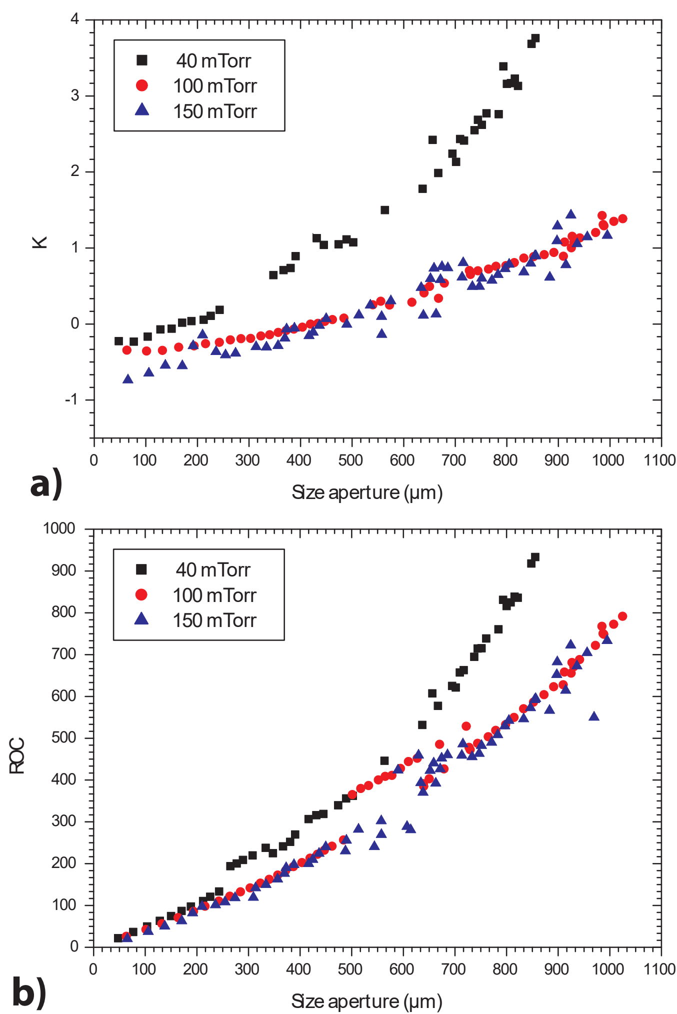

Figure 12. Conic constant of the specific size aperture.

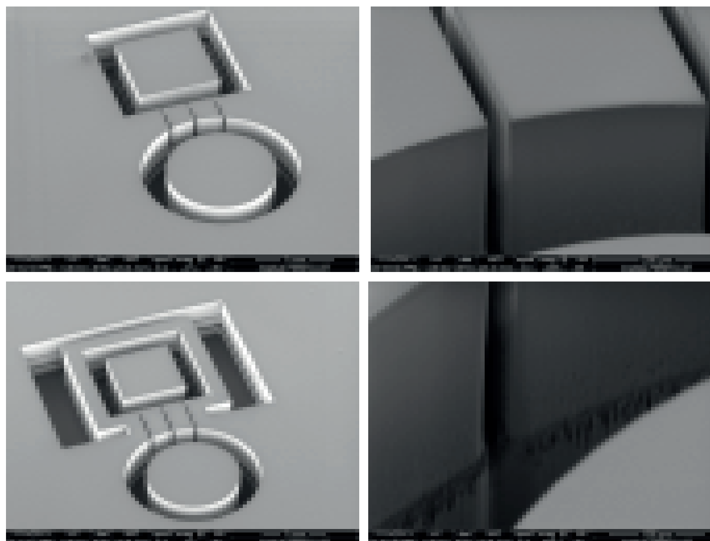

Figure 13. Fast ultra deep silicon 1.4 mm etched through caviite connected with microchannels.

Table 1. Different etch processes.

Parameters		Recipe 1	Recipe 2	Recipe 3
Pressure	(mTorr)	30	70	40
Coil Power	(Watts)	2500	2200	2000
Platen Power	(Watts)	20	20	20
Flow rate SF_6	(sccm)	400	500	500
Flow rate O_2	(sccm)	—	80	—
Flow rate C_4F_8	(sccm)	300	100	—
Chuck temperature	(C)	0	0	0
Mask Opening	(μm)	300		95
Etch depth	(μm)			121
Undercut	(μm)	1		52.4
Etch rate	(μm/min)	11	7	900
Selectivity$_{Si:Resist}$	(μm)	158:1	82:1	37:1
Anisotropy		1	0.7	—
Etch Profile		Vertical	Directional	Isotropic

Table 2. The Bosch process parameters for etching silicon by ICP-DRIE.

Recipe	Parameters	Passivation	Ion Bombardement	Etch
Recipe 1a	Process Time (s)	1.5-1.8	1.5-2	3
	Pressure (mTorr)	30	50	70
	Coil Power (Watts)	2500	2500	2500
	Platen Power (Watts)	20	150	25
	Flow rate SF_6 (sccm)	—	450	450
	Flow rate C_4F_8 (sccm)	300	—	—
Recipe 1b	Process Time (s)	1.2-1.5	1.3-1.5	2.5
	Pressure (mTorr)	40	30	30
	Coil Power (Watts)	2500	2500	2500
	Platen Power (Watts)	20	20	20
	Flow rate SF_6 (sccm)	—	400	400
	Flow rate C_4F_8 (sccm)	330	—	—

Table 3. Discussion and comparison between our work and previous research to manufacture the mold silicon by using a ICP-DRIE reactor.

Reference		Our work	[20]	[22]
Photoresist mask		AZ9260	NC	AZ9260
Mask Opening	(μm)	20-600	7-62	100-200
Chamber pressure	(mTorr)	40-150	10-70	17-27
Coil Power	(Watts)	2000	1000-3000	850
Platen Power	(Watts)	20	0-16	6-16
Flow rate SF_6	(sccm)	500	200-300	100
Flow rate Ar	(sccm)	–	–	40
Flow rate O_2	(sccm)	–	0-30	–
Chuck temperature	(C)	0	0-40	30
Etch time	(s)	900	300-750	120-300
Cavity depth	(μm)	27-290	28.6-100	75-260
RMS	(μm)	0.12-4	0.41-1.15	0.02-0.14